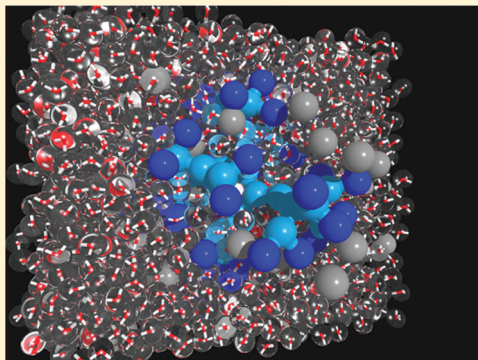


Explicit vs Implicit Water Simulations of Charged Dendrimers

Sebastian Huißmann,[†] Christos N. Likos, and Ronald Blaak*

Faculty of Physics, University of Vienna, Boltzmanngasse 5, A-1090 Vienna, Austria

ABSTRACT: Charged dendrimers with terminal or full charge of the nodes, single- or double-spacer, are simulated and a comparison is made between implicit and explicit water results. The main conclusion is that modeling the solvent with a continuum (dielectric constant $\epsilon_r = 80$) and ignoring its discrete nature results into a surprisingly accurate description of their properties. Sizes, density profiles and spacer dependence are reproduced within 10% at most. The counterion intake is overestimated by the implicit water model because in reality water intrudes all the way to the center and locally expels some counterions. The amount of water absorbed increases rapidly with charging the dendrimer.



1. INTRODUCTION

Dendrimers^{1,2} are very versatile macromolecules with a large number of technical and pharmaceutical applications. They are of great technological importance due to their role in for instance gene-delivery experiments,³ cancer treatment,⁴ or their use as contrast agents in biomedical imaging.⁵ Dendrimers are also interesting from a fundamental aspect.^{6–10} Their compactness and flexibility can be tuned by changing generation number and/or spacer length, which makes them an ideal model system, capable of bridging the gap between flexible polymers and hard spheres.¹¹

Advances in synthesis techniques have led to a large variety of dendritic architectures with many different key structural features.¹² Nowadays, the most commonly studied dendrimers are of the poly(amidoamine) (PAMAM) or poly(propylene-imine) (PPI) type. Dendrimers with acidic functional groups, synthesized by Newkome et al., were the first for which large size changes with pH variance have been observed for generation three (G3) dendrimers.¹² The change of the solution's pH value induces dissociation of ions into the solution, thereby charging the remaining molecule, which results in the electrostatic swelling of the latter. In a more systematic study, Young et al. compared dendrimers with acidic, neutral, or basic terminal functionality.¹³ They reported a maximum swelling of the hydrodynamic radius of 35% for the carboxylic acid- and amine-terminated dendrimers. However, alcohol-terminated dendrimers displayed no swelling or shrinking at all under pH change. Their results are consistent with the assumption that size variation arises from Coulombic repulsions between the charged monomers. Furthermore, they concluded that the finding of size variation as a function of pH should be general, provided the interior branches of the dendrimers are relatively flexible.¹³ The aforementioned discoveries formed the basis for experimental and simulation studies regarding the conformation of charged dendrimers and their possible use as encapsulation agents.

For polyelectrolyte chains and stars, it is well-known that charging them leads to dramatic changes in their size and conformations.^{11,14,15} It is therefore surprising that some controversy arose regarding the electrostatic swelling of high-generation dendrimers. Nisato et al. found in small angle neutron scattering (SANS) experiments that the size of a G8 PAMAM dendrimer is independent of charge density and ionic strength.¹⁶ On the contrary, Chen et al. found in their experiments on G6 dendrimers clear evidence for conformational changes and attributed the size invariance found by Nisato et al. to the dense packing of the G8 dendrimer.¹⁷ Moreover, pioneering simulation studies of dendrimers under varying ionic strength predicted a conformational change from dense-core to dense-shell.¹⁸ These contradictory observations led to many conjectures and debates on whether a charge-induced dendrimer swelling is completely absent or only diminished due to the very high steric crowding.^{11,16,17,19–24} A recent combined SANS and X-ray scattering study performed by Liu et al. clarified the microscopic behavior of charged polyelectrolyte dendrimers.²⁵ They provided conclusive evidence of the fact that high-generation PAMAM dendrimers undergo electrostatic swelling and conformational changes toward a denser-shell conformation upon protonation. A MD-simulation study of stiff and flexible dendritic polyelectrolytes not only confirmed their observations, but also showed that the flexibility of the dendrimer is of high importance for the understanding of conformational changes.²⁶ In line with these results is also the common use of dendrimers in gene-delivery experiments to make high generational PAMAM dendrimers more flexible by hydrolytic removal of some of their branches, which is necessary to maximize transfection efficiency.³ In recent small-angle neutron scattering experiments,²⁷ contrast variation was

Received: November 16, 2011

Revised: February 8, 2012

Published: February 22, 2012

employed to measure the monomer, counterion and water profiles of hydrophilic neutral and charged dendrimers. Once again, the growth of the dendrimer upon charging was confirmed, whereas at the same time the monomers maintain the dense-core configuration, i.e., significant back-folding exists also in the case of charging. Moreover, considerable water intake was found for the neutral dendrimer, which is further enhanced at low pH-values, for which the molecule is charged. The increase in size and water intake upon charging was also found in the simulation studies of Maiti et al.²⁸ and of Wu.²⁹

The size of the dendrimers being on the order of a few nanometers, is much smaller than that of a typical colloidal particle. The dendrimer's building blocks, the monomeric units consisting of, e.g., hydrocarbons, are of the same order of magnitude in size as water molecules. This makes a theoretical/computational treatment very time-consuming, since a large number of monomeric units and water molecules are involved. So what is required here, is an efficient computational technique that takes into account both the charge and the screening by the solvent—which is, in this case, water. It is therefore tempting to follow an implicit solvent approach. However, the granular nature of the solvent cannot always be neglected, since the formation of hydrogen bonds, the electrostatic interactions and hydrophobic attractions between nonpolar molecules might result in nontrivial effects. For example, Dzubiella et al. pointed out that taking into account the water molecules explicitly can cause the effect known as like-charge attractions between colloids.³⁰ Moreover, the very idea of screening via an effective dielectric constant ϵ requires averaging over many water molecules intervening between charges, which is not a priori guaranteed to be accurate at the microscopic scale.³¹

Previous MD-simulations have focused on charged PAMAM dendrimers in either implicitly or explicitly simulated water.^{22,28,29,32–37} However, a direct comparison of explicit vs implicit water simulation of charged dendrimers at different pH conditions is lacking up to now. In this work, we therefore examine the effects explicit/implicit water has on the conformational properties of a G4 dendrimer. The focus lies on the question of whether the screening character of water can be well approximated by an implicit solvent. We employ MD-simulations with the SPC/E model for water at ambient conditions and compare the results with the simulations of dendrimers in which the water is treated as an implicit continuum by means of the appropriate relative permittivity for the electrostatic interactions. Apart from a minor discrepancy of the counterion density in the core region of the dendrimer that can be attributed to steric interactions, we find that the static properties related to the conformational characterization of the dendrimers, can be accurately described by the implicit solvent approach.

The rest of this paper is organized as follows: The simulation model is described in section 2. We present our results in section 3 for dendrimers with and without spacer monomers between their branching nodes as a means of tuning their flexibility. A direct comparison shows that for charged dendrimers essentially the same behavior can be seen for implicit and explicit water. We summarize and draw our conclusions in section 4.

2. SIMULATION MODEL

We examine the conformations of 4th generation (G4) dendrimers and number of spacer segments P between the branching points, in solvents of varying pH by means of monomer-resolved MD simulations.^{38,39} A bead–spring model is used for

the dendrimers, where the monomers are modeled as beads in a united-atom approximation. The model dendrimers used in this work commence with two central beads that form the core, the so-called generation 0. By repeatedly linking two beads at each site, a new generation is formed. A dendrimer constructed this way has thus 2^{g+1} monomers or nodes per generation g , and since there are no spacer monomers between the nodes present this corresponds to having $P = 1$ spacer segments. When one spacer monomer is inserted between each of the nodes of the dendrimer, the number of spacer segments is $P = 2$. A G4-dendrimer has therefore 32 terminal monomers, a total of 62 nodes, and in the case of a dendrimer with $P = 2$ spacer segments, a total number of 123 monomers is present.

Dendrimers can be synthesized in such a fashion that the nodes become ionized at low pH values of the solution and remain neutral at high pH.¹¹ Furthermore, when monomeric units like primary and secondary amines are incorporated, a dendrimer can be obtained, such that only its terminal beads are charged at intermediate pH values.⁴⁰ A change in the pH value of the solution can therefore be modeled by charging the dendrimers in different fashions. Here, we restrict ourselves to terminally charged dendrimers, $Z = 32$, and fully charged dendrimers, $Z = 62$, with either $P = 1$ or $P = 2$ spacer segments.

We assume good solvent conditions for the monomers of the dendrimer. To this end, we employ a model of intermonomer interactions, in which each pair of beads at a relative distance r interacts via the purely repulsive, truncated and shifted Lennard-Jones⁴¹ potential:

$$V_{\text{LJ}}(r) = \begin{cases} 4\epsilon \left[\left(\frac{\sigma}{r}\right)^{12} - \left(\frac{\sigma}{r}\right)^6 + \frac{1}{4} \right], & r \leq 2^{1/6}\sigma \\ 0, & r > 2^{1/6}\sigma \end{cases} \quad (1)$$

where the interaction strength ϵ and the diameter σ fix the units of energy and length, respectively. A value of $\sigma = 4 \text{ \AA}$ has been chosen for the monomer diameter and $\epsilon = 0.19 \text{ kcal/mol}$ for the interaction parameter, which are reasonable values for hydrocarbons in a united-atom approximation.^{42,43}

The connectivity in the dendrimer, which is typically maintained by covalent chemical bonds, can be described by the so-called finite extensible nonlinear elastic (FENE) potential:⁴⁴

$$V_{\text{FENE}}(r) = \begin{cases} -U_0 \left(\frac{R_0}{\sigma}\right)^2 \ln \left[1 - \left(\frac{r}{R_0}\right)^2 \right], & r \leq R_0 \\ \infty, & r > R_0 \end{cases} \quad (2)$$

Here, U_0 is a measure for the spring constant and R_0 is the maximal bond-length between two monomers, for which we have chosen $U_0 = 15\epsilon$ and $R_0 = 1.5\sigma$, respectively.

The effective solvent simulations were performed using the Ewald summation method for the long-range Coulomb interactions between charged particles, given by

$$V_{\text{Coulomb}}(r) = \frac{e^2 Z_i Z_j}{\epsilon_r r} \quad (3)$$

with Z_i and Z_j the charge numbers, e the elementary charge, and ϵ_r the relative permittivity. The monomers are chosen to be either neutral or carrying positive monovalent charges. Overall charge neutrality is guaranteed by adding oppositely charged

counterions to the solution, which otherwise have the same steric interactions as neutral monomers. For the solvent, water at room temperature ($T = 293$ K) is chosen. Only the screening of the electrostatic interactions caused by water is modeled in the implicit solvent simulations, by imposing $\epsilon_r = 80$.

A large number of effective models have been used for the simulation of liquid water. The computational cost rises with the number of charged sites that is included in the various models. Moreover, a distinction can be made between rigid^{45,46} and flexible^{47,48} models, where the OH-bond interaction in the latter case is described by a harmonic or anharmonic potential. A frequently used three-site model is the extended simple point charge (SPC/E) model.⁴⁸ This model is easy to implement; it consists of only three sites, and has therefore a relatively low computational cost as compared to other more complex ones. Nevertheless, it reproduces many of the properties of liquid water at ambient conditions with reasonable accuracy. For example, the dielectric constant is found to be 75 ± 7 for SPC/E under ambient conditions.⁴⁹

A single SPC/E water molecule is represented by a spherical particle with three charged sites, one oxygen (O) atom in the center and two hydrogen (H) atoms. The H atoms are bound to the O-site by an anharmonic interaction with equilibrium length l_0 and interaction constants k_l and k_{cub} . The OH-bond potential is given by

$$V_{OH}(l) = k_l(l - l_0)^2 + k_l k_{cub} (l - l_0)^3 \quad (4)$$

where l is the distance between an O and either of the H atoms of the same molecule. The H–O–H angle θ is constraint via a harmonic angle potential,

$$V_{HOH}(\theta) = k_\theta(\theta - \theta_0)^2 \quad (5)$$

where θ_0 is the equilibrium bond angle and spring constant k_θ .

The non-Coulombic intermolecular interaction between SPC/E water molecules consists only of a Lennard-Jones interaction between two O-sites at a relative distance r ,

$$V_{OO}(r) = \frac{A}{r^{12}} - \frac{B}{r^6} \quad (6)$$

The dipolar nature of the water molecules is modeled with partial charges for the O and H atoms, given by q_O and q_H , respectively. Coulomb interactions between charged sites are calculated between distinct water molecules only. All Coulomb interactions in the explicit water simulations are modeled via eq 3 with $\epsilon_r = 80$. For completeness, the full parameter set of the SPC/E model by Ferguson⁴⁹ is given in Table 1.

From a comparison of eq 6 with the form of the Lennard-Jones potential,

$$V_{LJ}(r) = 4\epsilon \left[\left(\frac{\sigma}{r} \right)^{12} - \left(\frac{\sigma}{r} \right)^6 \right] \quad (7)$$

one obtains a diameter $\sigma_w = 3.183$ Å and an interaction strength $\epsilon_w = 0.166$ kcal/mol for the water molecule. All neutral and charged particles interact with the O atom of a water molecule

via the Lennard-Jones potential eq 7. The corresponding parameters are calculated from the Lorentz–Berthelot mixing rules,

$$\epsilon_{\alpha\beta} = \sqrt{\epsilon_\alpha \epsilon_\beta} \quad (8)$$

for the interaction strength, and

$$\sigma_{\alpha\beta} = 0.5(\sigma_\alpha + \sigma_\beta) \quad (9)$$

for the molecular diameter, where α and β correspond to any type of particle in the system, being a neutral or charged monomers, counterion or the O-site of a SPC/E water molecule.

A word of caution should be mentioned regarding the modeling of the monomer–monomer interactions in the implicit- and explicit water simulations. In our work, we have taken *the same* monomer–monomer interaction potential for both cases, namely the truncated-and-shifted (purely repulsive) Lennard-Jones potential of eq 1. Strictly speaking, this is not correct. The purely repulsive monomer–monomer potential employed in the implicit water simulation is itself an effective interaction with results from the combined effect of the bare monomer–monomer potential $\tilde{v}_{mm}(r)$ and the water molecules, which have been traced out. The bare potential $\tilde{v}_{mm}(r)$, which is not purely repulsive but rather of the Lennard-Jones type, should be the one to be employed in the explicit water simulations. However, we do not know which precise form of this potential would give rise, upon tracing out the solvent, to the truncated-and-shifted Lennard-Jones potential which is commonly employed in almost all implicit-water simulations. We argue here that the precise form of $\tilde{v}_{mm}(r)$ should not be important, though. As far as the charged monomers are concerned, the unscreened ($\epsilon_r = 1$) Coulomb interaction is strongly repulsive and thus renders the weak, short-range attractions between monomers irrelevant. Concerning the neutral monomers, which are found in the interior of terminally charged dendrimers, we argue that their strong hydrophilicity will result into substantial water intake, as it has been confirmed both by previous simulations^{28,29} and in experiments.²⁷ Under these conditions, and given the tendency of water molecules to form clusters and connected groups, any two neutral monomers will almost always be found to be separated by intervening water molecules, so that the attractions present in $\tilde{v}_{mm}(r)$ will not be relevant. Accordingly, we adopt the simplest possible approach by assuming pure steric repulsions between monomers, modeled in an identical way in both the implicit and the explicit water approaches. This is also similar to the approach of Gurtovenko et al.,³⁵ who performed simulations of charged dendrimers in explicit, nonpolar solvents, employing also a truncated-and-shifted Lennard-Jones interaction between the monomers. A proper, microscopic, and substance-specific treatment of this coarse-graining step is also possible by means of *ab initio* techniques that commence at a quantum-mechanical level and proceed to the derivation of molecular-mechanical (MM) force fields.^{50–52} However, this is beyond the scope of our work, which focuses on more generic aspects. Besides, the form of the MM-force is not uniquely determined but it rather depends on the original,

Table 1. Parameter Set^a for the SPC/E Model Taken from Ferguson et al.⁴⁹

k_l	k_{cub}	l_0	k_θ	θ_0	A	B	q_H	q_O	m_H	m_O	m_M
547.5	-1.65	1.0	49.9	109.5	650 000	625.47	0.413	-0.826	1	16	14

^aEnergies are given in kcal/mol, lengths in Å, angles in radians, masses in u, and the partial charges in electron units. The symbol m_M denotes the monomer mass.

quantum-mechanical quantities that should be matched by this field, see ref 50 for details.

For bulk water at room temperature and normal pressure, the nonpolarizable SPC/E model reproduces many of the properties of water with similar accuracy as other very good rigid and more complex models.^{46,53} Moreover, simulation studies of polarizable water models have shown that polarization effects are of secondary importance at hydrophobic and other surfaces.^{54–56} A temperature of $T = 293$ K has been maintained by applying the Berendsen thermostat⁴⁷ to the explicitly simulated solvent only, in order to avoid artifacts such as the hot-solvent/cold-solute problem.⁵⁷ For the implicit solvent simulation, the Andersen thermostat⁵⁸ has been used. The simulation box was chosen to be a cube with sides $L = 48$ Å and periodic boundary conditions. For the explicit water simulations 3678 water molecules have been used, a choice which corresponds to assuming normal pressure at the imposed water temperature. In the case of the $P = 1$ dendrimers, this is sufficient to guarantee that they do not interact with their own image. For the $P = 2$ dendrimers the same box size is used for computational reasons, but it should be noted that it is now comparable to the maximum extension of the dendrimers. Consequently, these dendrimers are simulated at a non-negligible, finite density. The MD equations of motion were integrated with a time step of $\delta t = 1.25$ fs. Initial configurations have been equilibrated for about $t_{\text{eq}} = 400$ ps, which is sufficiently long for the counterions to diffuse into the core of the dendrimer and to reach a steady state for the in- and out-flux. After equilibration, the simulations were run for $t_{\text{run}} = 1.25$ ns to obtain good statistics for the measurements. In terms of the natural time unit in the implicit water simulations, $\tau = (m_M \sigma^2 / \varepsilon)^{1/2}$, introducing the values $\varepsilon = 0.19$ kcal/mol, $\sigma = 4$ Å, and $m_M = 14u$ employed here, $\tau = 1.68$ ps obtains, yielding $\delta t = 7.5 \times 10^{-4}\tau$, and subsequent times $t_{\text{eq}} = 240\tau$ for equilibration, as well as $t_{\text{run}} = 750\tau$ for measurements.

3. RESULTS

Simulation snapshots of $P = 1$ dendrimers with charged end-groups, $Z = 32$, and with all nodes charged, $Z = 62$, are shown in Figure 1 for explicitly and implicitly simulated water. In all cases, the charged dendrimers have a more open conformation as compared to a neutral dendrimer that looks rather compact (not shown). This is mainly due to the Coulombic interaction between the charged monomers. At the same time, counterions are absorbed by the dendrimers, thereby screening the electrostatic repulsion to some extent. Although the fractions of neutral and charged particles are almost the same, the water molecules are found also within the terminally charged dendrimer structure, as illustrated in Figure 1a. This suggests that these dendrimers are soluble in aqueous solutions. The formation of hydrogen-bonds between the dendrimer's terminal moieties and the water molecules, however, results in a larger energy gain than the formation of bonds between water molecules in the bulk. Consequently, the water density at their periphery is increased with respect to that of hydrophobic solutes.³⁰ This effect leads to an enlarged separation between the charged monomers, in addition to the one already caused by the electrostatic repulsions. Similar considerations hold for the fully charged dendrimer, shown in Figure 1 (c), (d) for explicitly and implicitly simulated water, respectively. Here of course, no hydrophobic core is involved, since all monomers are charged.

Because no differences in the dendrimer's conformations can be discerned from the snapshots, a more detailed analysis is necessary. Information about the size changes can be obtained by considering the radius of gyration, R_g , of the dendrimers, which can be measured by SANS, X-ray, or static-light scattering experiments, and is given by

$$R_g^2 = \left\langle \frac{1}{N} \sum_{i=1}^N (\mathbf{r}_i - \mathbf{r}_c)^2 \right\rangle \quad (10)$$

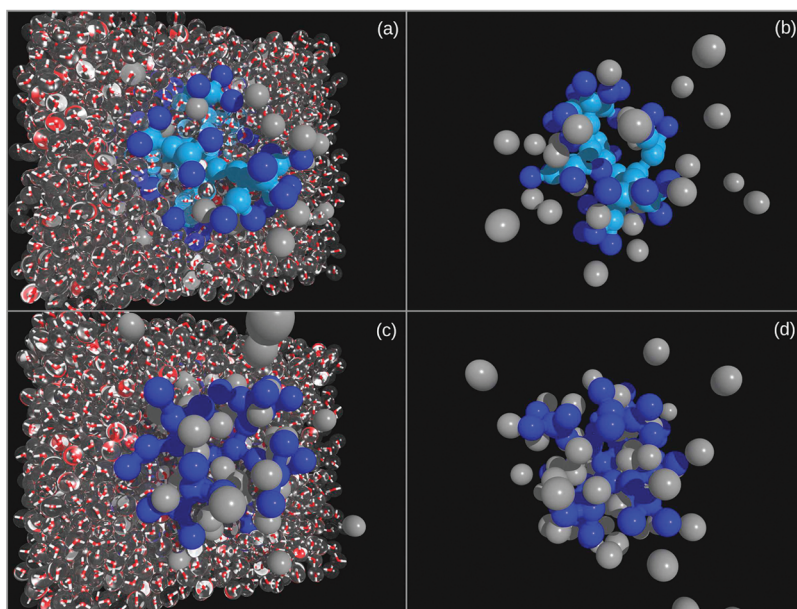


Figure 1. Snapshots from simulations of $P = 1$ dendrimers with $Z = 32$ (a, b), and $Z = 62$ (c, d) in explicitly and implicitly simulated water, respectively. Charged monomers of the dendrimer are shown in dark blue, neutral monomers in light blue and counterions in gray color. The water molecules are shown as transparent spheres, where the oxygen position is indicated by red and that of the hydrogens by white colors. The diameter of the spheres are σ and σ_w for the monomer/ions and water molecules, respectively.

where N is the number of monomers, \mathbf{r}_i the position of the i th monomer, and \mathbf{r}_c the position vector of the center of mass of the dendrimer. Simulation results are shown in Table 2. The

Table 2. Radius of Gyration, R_g , Measured in Units of the Monomer Diameter σ for Dendrimers with $P = 1$ and $P = 2$ Spacer Segments in Explicitly and Implicitly Simulated Water^a

Z	explicit water		implicit water	
	$P = 1$	$P = 2$	$P = 1$	$P = 2$
32	2.80	3.87	2.72	4.14
62	3.23	4.57	2.95	4.44

^aThe error is on the order of 0.01σ in all cases.

size of the $P = 1$ dendrimers is larger for explicitly simulated water than for implicit water, for both the terminally charged and fully charged dendrimers. The increase in the number of neutral monomers by the insertion of spacers diminishes the growth in size of the dendrimers upon charging, because of the additional effective attractions between them that are induced by the solvent. The relative size increase of the dendrimers upon lowering the pH, is in good quantitative agreement with experiments.^{12,13,24,25,27} This illustrates that although an oversimplified simulation model without detailed atomistic information is employed here, it is sufficient to capture the essential features and understand the basic conformational properties of dendrimers.

In order to gain a better understanding of the intramolecular structure the density profiles of the node monomers and of the counterions have been measured with respect to the center of mass \mathbf{r}_c

$$\rho(r) = \left\langle \sum_{i=1}^N \delta(\mathbf{r} - \mathbf{r}_i + \mathbf{r}_c) \right\rangle \quad (11)$$

where \mathbf{r}_i denotes the position of the i th particle from the total number of particles N , which can be either nodes or counterions.

The density profiles of the node monomers, $\rho_n(r)$, and of the counterions, $\rho_c(r)$, are shown in Figure 2 for the $P = 1$ dendrimer. For the terminally charged dendrimers, see Figure 2 (a), the density distributions of the monomers with explicitly and implicitly simulated water almost coincide. However, in the case of explicit water the shell structure of the dendrimer is more pronounced. This is also the case for the fully charged dendrimers, as shown in Figure 2c. In addition, the peaks are shifted outward with respect to the center, which is explained by water molecules being absorbed into the core of the dendrimer. This is in fact a simple scaling, which becomes apparent from the inset where both profiles are shown as a function of the distance $x = r/R_g$ to the center in terms of the radius of gyration R_g . The fact that the monomer density profiles stemming from the implicit and explicit water simulations collapse onto the same curve for either dendrimer, illustrates that the implicit simulations are capable of reproducing the salient characteristics of (partially) charged dendrimers.

The counterion distributions are shown in Figure 2, parts b and d, for the terminally and fully charged dendrimers, respectively. These profiles are slightly more structured when the water molecules are simulated explicitly. The open dendrimer structure allows counterions to diffuse into the center of the molecule, only to be expelled from a small region near the center of mass due to its closeness to the central pair of generation 0 monomers. Since the monomer density profiles are very similar, the fact that counterion density in the case of explicit water is somewhat lower as well as more structured can only be attributed to the presence of water molecules.

The measured density distributions of node monomers and counterions for the $P = 2$ dendrimer are shown in Figure 3. The overall structure in these profiles is less pronounced compared to those of the $P = 1$ dendrimers, which is caused by the additional freedom and flexibility by the additional spacer. The terminally charged dendrimer in Figure 3a is more compact in

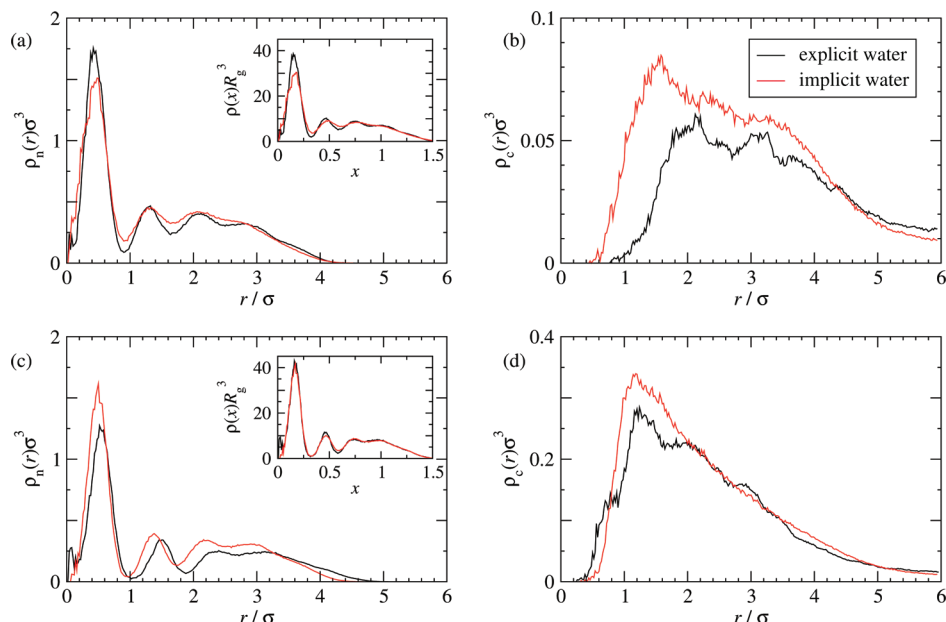


Figure 2. Radial density distribution of node monomers, $\rho_n(r)$, (a, c) and counterions, $\rho_c(r)$, (b, d) as a function of the distance, r , from the center of mass for the $P = 1$ dendrimer. The dendrimer's and counterion's total charge is $Z = 32$ (a, b) and $Z = 62$ (c, d). The insets show the distribution of node monomers but with the radius of gyration, R_g , as the reference length scale.

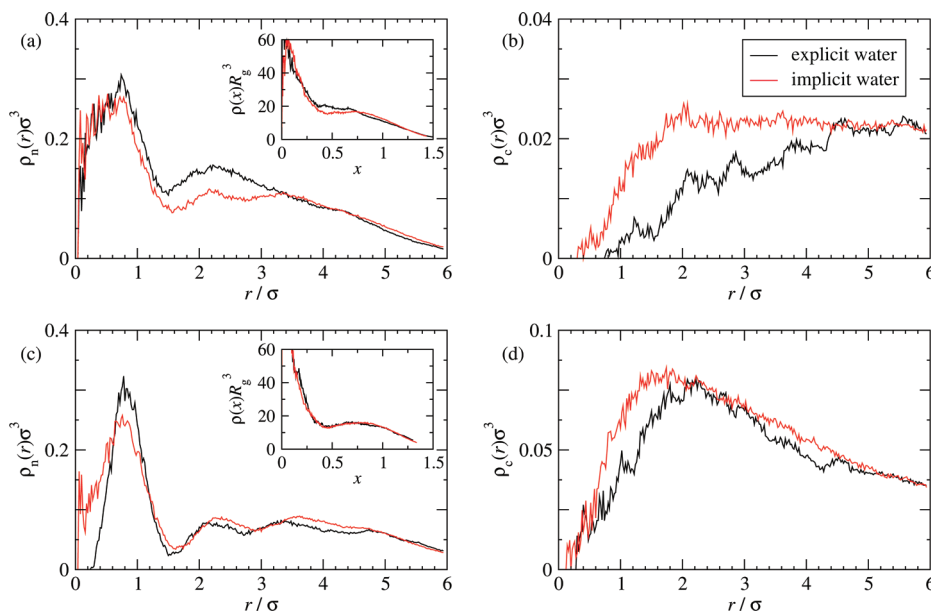


Figure 3. Radial density distribution of node monomers, $\rho_n(r)$, (a, c) and counterions, $\rho_c(r)$, (b, d) as a function of the distance, r , from the center of mass for the $P = 2$ dendrimer. The dendrimer's and counterion's total charge is $Z = 32$ (a, b) and $Z = 62$ (c, d). The insets show the combined distribution of node monomers and spacers as a function of the scaled distance $x = r/R_g$. Note that the insets show the total monomer profile, including the spacers, whereas the main plots only the nodes, thus the two are not scaled versions of one another.

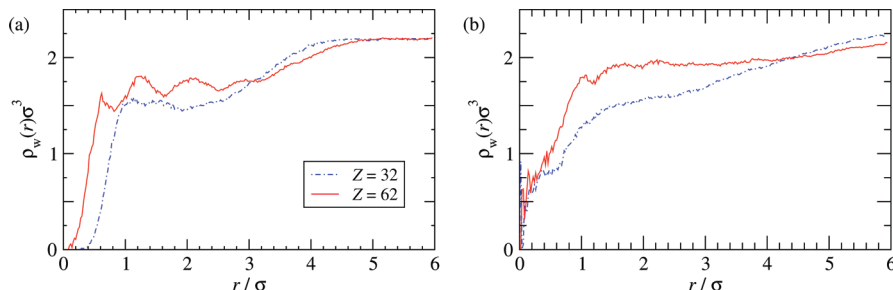


Figure 4. Radial distribution of water molecules, $\rho_w(r)$, as a function of the distance, r , from the center of mass for dendrimers with (a) $P = 1$ and (b) $P = 2$ spacer segments.

explicit water, which is due to the hydrophobically induced attraction between the neutral monomers of the lower generations, which is missing in the implicit water simulation. At the same time the counterions, as shown in Figure 3b, are expelled from the dendrimer's interior. The leveling off of these profiles is caused by the finite dendrimer density that is being used. The nodes of the fully charged dendrimer, Figure 3c, show good agreement between explicit and implicit water both with respect of the position of the peaks and their heights. However, the structure-stabilizing effect of the water, absorbed into the dendrimer is clearly visible here, as indicated by expulsion of monomers from the region around the center of mass. The combined density profiles of node monomers and spacers are shown in the insets with the radius of gyration as the reference length scale. Similar as in the case of the $P = 1$ dendrimers, the scaled profiles coincide.

A quantity that is experimentally accessible is the number of water molecules absorbed by the dendrimer.⁵⁹ The water distributions, $\rho_w(r)$, of the $P = 1$ and $P = 2$ dendrimers in the explicit water simulations are shown in Figure 4, parts a and b, respectively. In both cases, more water is absorbed the higher the charge of the dendrimers. Combined with the observation that the shell structure of the fully charged dendrimer without spacer is imposed on the water distribution, this supports the

picture sketched above that it is preferential for the water molecules to bind to the charged monomers. The additional steric interactions between charged monomers and water provide the basis for the anticorrelation between the profiles in the interior. In the periphery of the molecule, the distance between charged sites is large enough to avoid the necessity of following that shell structure. For the dendrimers with an additional spacer this is even the case for the lower generation nodes, because of the additional available volume they provide. Also note that they facilitate the diffusion of water and counterions to the core and allow them to reach the center of mass for the $P = 2$ dendrimers. Our findings are consistent with experimental results from SANS measurements,²⁷ where very substantial water intake within the interior of neutral dendrimers was found, and which was further enhanced by charging the molecules. Though we have not simulated a completely neutral dendrimer in our case but rather terminally charged (as well as fully charged) ones, the trend is the same: upon additional charging, more water molecules are absorbed to the interior of the dendrimer. The same feature was also seen in the simulations of Maiti et al.,²⁸ who employed explicit water models, as well as in the work of Gurtovenko et al.³⁵ In the latter case, however, the solvent particles were modeled as apolar beads and the charging

by modification of the Bjerrum length, which has no direct correspondence with our approach.

In order to quantify the amount of absorbed water the number of water molecules within a sphere of radius R_g around the center of mass have been measured, see Table 3. The

Table 3. Water Intake Obtained by integrating the radial water distribution up to R_g

Z	P = 1	P = 2
32	137	412
62	242	779

amount of absorbed water is almost doubled upon going from a terminally to a fully charged dendrimer for the $P = 1$ as well as the $P = 2$ case. This illustrates again that the water intake is strongly correlated with the total charge of the dendrimer. However, due to the relatively small amount of free space within the $P = 1$ dendrimer the density of water is somewhat lower than that of the dendrimer with $P = 2$ spacer segments.

4. DISCUSSION AND CONCLUSIONS

We investigated the effect that the discrete nature and the dielectric properties of an aqueous solution have on the conformations of dendrimers. Electrostatic interactions between charged entities constitute the main contribution to the conformation of the dendrimers in all studied cases here. The absorbed water molecules do result in some additional steric interactions, which cause the dendrimers to swell more than one might expect on the basis of their screened Coulomb interactions. In addition, it causes minor rearrangements of the counterions internally. These differences are however small, hence simulating the water molecules explicitly is only of secondary importance for the terminally or fully charged dendrimers considered here. We have shown that the equilibrium properties of charged dendrimers are very weakly sensitive on the explicit water against continuum water modeling of the solvent. This holds for the monomer and the counterion density profiles, for the ordering of the generations and the existence of voids in the structure (as witnessed by the minima in the density profiles). In addition, we have shown that when the density profiles are scaled on the gyration radius, i.e., when the dendrimers are seen at a mesoscopic scale, the profiles from the two approaches collapse onto one another. Given the known fact that a further coarse-graining of the dendrimers, i.e., the derivation of a dendrimer–dendrimer effective interaction^{60,61} crucially depends on the form of these profiles, it can be asserted that the latter will be insensitive to the modeling of the aqueous solvent as a dielectric continuum although there is no *a priori* guarantee for this to be the case. Therefore, there are reasons to believe that a host of equilibrium properties of dendrimers or concentrated solutions of the same can be calculated in continuum solvent simulation models, which are much faster than their explicit water counterparts.

The usage of the implicit water model for athermal solvents is well suited for the description of (partially) charged dendrimers and can be controlled via the adjustment of the relative permittivity. A very good agreement between implicit and explicit water simulation, as seen by the collapse of the density profiles when suitably scaled, is found. However, the deviations increase when more neutral monomers are included into the dendrimer, i.e., when hydrophobic effects start playing an increasingly important role. Finally, we emphasize that the work

presented here is focused on the static properties, related to dendrimer conformations. In previous works employing explicit solvent models,^{33,35} the dynamics of water and/or the dendrimer branches was also studied. Although it would have been possible to do the same here and provide a comparison with the previous results, this would lie clearly outside the scope of this work, which is to provide a comparison between implicit and explicit solvent models. Such a comparison makes little sense when dynamical quantities are concerned, since the whole dynamics changes when solvent is eliminated: the Newtonian equations of motion at the solvent-resolved level turn into a Langevin dynamics, including friction and possible hydrodynamic effects when the solvent is integrated out. Otherwise, if one employs the same dynamics at both scales, an enormous acceleration of the dynamics results at the coarse-grained level, as is well-known also for other soft systems.⁶² A study of the effects of multivalent counterions on the internal dynamics of dendrimers, which has direct connections with recent simulations³⁶ and experiments⁶³ will be the subject of future work.

■ AUTHOR INFORMATION

Corresponding Author

*E-mail: ronald.blaak@univie.ac.at

Notes

The authors declare no competing financial interest.

Present Address

[†]Institute for Computational Molecular Science and Department of Chemistry, Temple University, Philadelphia, Pennsylvania 19122, United States.

■ ACKNOWLEDGMENTS

This work has been supported by the CMS Vienna and by the Marie Curie Training Network ITN-COMPLOIDS, FP7-PEOPLE-ITN-2008, Project No. 234810.

■ REFERENCES

- (1) Buhleier, G. E.; Wehner, W.; Vögtle, F. *Synthesis (Stuttgart)* **1978**, 2, 155.
- (2) Tomalia, D. A.; Naylor, A. M.; Goddard, W. A. *Angew. Chem., Int. Ed. Engl.* **1990**, 29, 138–175.
- (3) Dennig, J. *Dendrimers V*; Springer: Berlin and Heidelberg, Germany, 2003; Vol. 228; pp 621–672.
- (4) Choi, Y. S.; Thomas, T.; Kotlyar, A.; Islam, M. T.; Baker, J. R. Jr. *Chem. Biol.* **2005**, 12, 35–43.
- (5) Stiriba, S. E.; Frey, H.; Haag, R. *Angew. Chem., Int. Ed. Engl.* **2002**, 41, 1329–1334.
- (6) Harreis, H. M.; Likos, C. N.; Ballauff, M. *J. Chem. Phys.* **2003**, 118, 1979–1988.
- (7) Rosenfeldt, S.; Dingenouts, N.; Ballauff, M.; Lindner, P.; Likos, C. N.; Werner, N.; Vögtle, F. *J. Macromol. Chem. Phys.* **2002**, 203, 1995–2004.
- (8) Pötschke, D.; Ballauff, M.; Lindner, P.; Fischer, M.; Vögtle, F. *Macromolecules* **1999**, 32, 4079.
- (9) Pötschke, D.; Ballauff, M.; Lindner, P.; Fischer, M.; Vögtle, F. *Macromol. Chem. Phys.* **2000**, 201, 330.
- (10) Rissanou, A. N.; Economou, I. G.; Panagiotopoulos, A. Z. *Macromolecules* **2006**, 39, 6298–6305.
- (11) Ballauff, M.; Likos, C. N. *Angew. Chem., Int. Ed. Engl.* **2004**, 43, 2998–3020.
- (12) Newkome, G. R.; Young, J. K.; Baker, G. R.; Potter, R. L.; Audoly, L.; Cooper, D.; Weis, C. D. *Macromolecules* **1993**, 26, 2394–2396.
- (13) Young, J. K.; Baker, G. R.; Newkome, G. R.; Morris, K. F.; Johnson, C. S. Jr. *Macromolecules* **1994**, 27, 3464–3471.
- (14) Jusufi, A.; Likos, C. N. *Rev. Mod. Phys.* **2009**, 81, 1753–1772.

- (15) Likos, C. N. *Phys. Rep.* **2001**, *348*, 267–439.
- (16) Nisato, G.; Ivkov, R.; Amis, E. J. *Macromolecules* **2000**, *33*, 4172.
- (17) Chen, W.; Tomalia, D. A.; Thomas, J. L. *Macromolecules* **2000**, *33*, 9169–9172.
- (18) Welch, P.; Muthukumar, M. *Macromolecules* **1998**, *31*, 5892–5897.
- (19) Likos, C. N.; Ballauff, M. *Functional Molecular Nanostructures; Topics in Current Chemistry* 245; Springer: Berlin and Heidelberg, Germany, 2005; pp 239–252.
- (20) Chen, W.-R.; Porcar, L.; Liu, Y.; Butler, P. D.; Magid, L. J. *Macromolecules* **2007**, *40*, 5887–5898.
- (21) Giupponi, G.; Buzzo, D. M. A.; Adolf, D. B. *Macromolecules* **2007**, *40*, 5959–5965.
- (22) Liu, Y.; Bryantsev, V. S.; Diallo, M. S.; Goddard, W. A. III. *J. Am. Chem. Soc.* **2009**, *131*, 2798–2799.
- (23) Blaak, R.; Lehmann, S.; Likos, C. N. *Macromolecules* **2008**, *41*, 4452–4458.
- (24) Porcar, L.; Hong, K.; Butler, P. D.; Herwig, K. W.; Smith, G. S.; Liu, Y.; Chen, W.-R. *J. Phys. Chem. B* **2010**, *114*, 1751–1756.
- (25) Liu, Y.; Chen, C.-Y.; Chen, H.-L.; Hong, K.; Shew, C.-Y.; Li, X.; Liu, L.; Melnichenko, Y. B.; Smith, G. S.; Herwig, K. W.; Porcar, L.; Chen, W.-R. *J. Phys. Chem. Lett.* **2010**, *1*, 2020–2024.
- (26) Huißmann, S.; Likos, C. N.; Blaak, R. *J. Mater. Chem.* **2010**, *20*, 10486–10494.
- (27) Wu, B.; Li, X.; Do, C.; Kim, T.-H.; Shew, C.-Y.; Liu, Y.; Yang, J.; Hong, K.; Porcar, L.; Chen, C.-Y.; Liu, E.; Smith, G.; Herwig, K.; Chen, W.-R. *J. Chem. Phys.* **2011**, *135*, 144903.
- (28) Maiti, P. K.; Çağın, T.; Lin, S.-T.; Goddard, W. A. III. *Macromolecules* **2005**, *38*, 979.
- (29) Wu, C. *Mol. Simulat.* **2010**, *36*, 1164.
- (30) Dzubiella, J.; Hansen, J.-P. *J. Chem. Phys.* **2003**, *119*, 12049.
- (31) Dzubiella, J.; Swanson, J. M. J.; McCammon, J. A. *J. Chem. Phys.* **2006**, *124*, 084905.
- (32) Lee, I.; Athey, B. D.; Wetzel, A. W.; Meixner, W.; Baker, J. R. Jr. *Macromolecules* **2002**, *35*, 4510–4520.
- (33) Lin, S.-T.; Maiti, P. K.; Goddard, W. A. III. *J. Phys. Chem. B* **2005**, *109*, 8663.
- (34) Maiti, P. K.; Goddard, W. A. III. *J. Phys. Chem. B* **2006**, *110*, 25628–25632.
- (35) Gurtovenko, A. A.; Lyulin, S. V.; Karttunen, M.; Vattulainen, I. *J. Chem. Phys.* **2006**, *124*, 8.
- (36) Tian, W.-D.; Ma, Y.-Q. *Soft Matter* **2010**, *6*, 1308.
- (37) Zhong, T.; Ai, P.; Zhou, J. *Fluid Phase Equilib.* **2010**, *302*, 43.
- (38) Frenkel, D.; Smit, B. *Understanding Molecular Simulation*; Academic Press: San Diego, CA, 1996.
- (39) Allen, M. P.; Tildesley, D. J. *Computer Simulation of Liquids*; Clarendon Press: Oxford, U.K., 1989.
- (40) Cakara, D.; Kleinmann, J.; Borkovec, M. *Macromolecules* **2003**, *36*, 4201–4207.
- (41) Weeks, J.; Chandler, D.; Andersen, H. *J. Chem. Phys.* **1971**, *54*, 5237.
- (42) Jorgensen, W. L.; Madura, J. D.; Swenson, C. J. *J. Am. Chem. Soc.* **1984**, *106*, 6638–6646.
- (43) Götze, I. O.; Harreis, H. M.; Likos, C. N. *J. Chem. Phys.* **2004**, *120*, 7761–7771.
- (44) Grest, G. S.; Kremer, K.; Witten, T. A. *Macromolecules* **1987**, *20*, 1376–1383.
- (45) Jorgensen, W. L.; Chandrasekhar, J.; Madura, J. D.; Impey, R. W.; Klein, M. L. *J. Chem. Phys.* **1983**, *79*, 926.
- (46) Bagchi, K.; Balasubramanian, S.; Klein, M. L. *J. Chem. Phys.* **1997**, *107*, 8561–8567.
- (47) Berendsen, H. J. C.; Postma, J. P. M.; van Gunsteren, W. F.; DiNola, A.; Haak, J. R. *J. Chem. Phys.* **1984**, *81*, 3684.
- (48) Berendsen, H. J. C.; Grigera, J. R.; Straatsma, T. P. *J. Phys. Chem.* **1987**, *91*, 6269–6271.
- (49) Ferguson, D. M. *J. Comput. Chem.* **1995**, *16*, 501–511.
- (50) Lyubartsev, A.; Mirzoef, A.; Chen, L.-J.; Laaksonen, A. *Faraday Discuss.* **2010**, *144*, 43.
- (51) Lyubatsev, A. P.; Laaksonen, A. *J. Chem. Phys.* **1999**, *111*, 11207.
- (52) Lyubatsev, A. P.; Laaksonen, A. *Phys. Rev. E* **1995**, *52*, 3730.
- (53) Kusalik, P. G.; Svishchev, I. M. *Science* **1994**, *265*, 1219.
- (54) Wallqvist, A. *Chem. Phys. Lett.* **1990**, *165*, 437.
- (55) Kohlmeyer, A.; Witschel, W.; Spohr, E. *Chem. Phys.* **1996**, *213*, 211–216.
- (56) Bresme, F.; Wynveen, A. *J. Chem. Phys.* **2007**, *126*, 044501.
- (57) Lingenheil, M.; Denschlag, R.; Reichold, R.; Tavan, P. *J. Chem. Theory Comput.* **2008**, *4*, 1293–1306.
- (58) Andersen, H. C. *J. Chem. Phys.* **1980**, *72*, 2384.
- (59) Li, T. K.; Hong, K.; Porcar, L.; Verduzco, R.; Butler, P. D.; Smith, G. S.; Liu, Y.; Chen, W.-R. *Macromolecules* **2008**, *41*, 8916–8920.
- (60) Tian, W.-D.; Ma, Y.-Q. *Soft Matter* **2011**, *7*, 500.
- (61) Huißmann, S.; Blaak, R.; Likos, C. N. *Soft Matter* **2011**, *7*, 8419.
- (62) Lopez, C. F.; Moore, P. B.; Shelley, J. C.; Shelley, M. Y.; Klein, M. L. *Comput. Phys. Commun.* **2002**, *147*, 1.
- (63) Li, X.; Zamponi, M.; Hong, K.; L.; Porcar, C.-Y. S.; Jenkins, T.; Liu, E.; Smith, G. S.; Herwig, K. W.; Liu, Y.; Chen, W.-R. *Soft Matter* **2011**, *7*, 618–622.